

Under the different pump power, the FWHM and peak power of the generated pulse increase in direct ratio with the pump power, as shown in Figure 4, where the solid line denotes the linear fit for FWHM with a slope of 0.02 ns/mW, and the dashed line denotes the linear fit for the peak power with a slope of 0.01 V/mW.

Finally, using a length of 5-m PMF, the experiment is repeated, and multiwavelength comb generated can also be achieved. The only difference is the wavelength spacing between neighboring peaks (0.98 nm), which is determined by the length of PMF.

4. CONCLUSION

In conclusion, we have experimentally demonstrated multiwavelength comb generation in an all-fiber self-starting passively mode-locked figure-eight erbium-doped fiber laser. A nonlinear optical-loop mirror (NOLM), consisting of a symmetrical coupler and long SMF, can act as saturable absorber for nonlinear switching through nonlinear polarization rotation. An equivalent Lyot birefringent filter consisting of PMF and polarization dependent isolator can implement linear filtering.

ACKNOWLEDGMENTS

The authors acknowledge support from the National Natural Science Foundation of China under the grant nos. 60577048/10474064, and the Science and Technology Committee of Shanghai Municipal under contract nos. 022261003/04DZ14001.

REFERENCES

1. J. Chow, G. Town, B. Eggleton, M. Ibsen, K. Sugden, and I. Bennion, Multiwavelength generation in an erbium-doped fiber laser using in-fiber comb filters, *IEEE Photon Technol Lett* 8 (1996), 60–62.
2. G. Das and J.W.Y. Lit, Multiwavelength fiber laser using a Sagnac loop filter, *Microwave Opt Technol Lett* 36 (2003), 200–202.
3. G.J. Cowle and D.Y. Stepanov, Multiple wavelength generation with Brillouin/erbium fiber lasers, *IEEE Photon Technol Lett* 8 (1996), 1465–1467.
4. H. Takara, T. Ohara, K. Mori, K.I. Sato, E. Yamada, Y. Inoue, T. Shibata, M. Abe, T. Morioka, and K. Sato, More than 1000 channel optical frequency chain generation from single supercontinuum source with 12.5-GHz channel spacing, *Electron Lett* 36 (2000), 2089–2090.
5. E.A. Kuzin, B.I. Escamilla, D.E. Garcia-Gomez, and J.W. Haus, Fiber laser mode locked by a Sagnac interferometer with nonlinear polarization rotation, *Opt Lett* 26 (2001), 1559.
6. E.A. Kuzin, J.A. Andrade-Lucio, B.I. Escamilla, R. Rojas-Laguna, and J. Sanchez-Mondragon, Nonlinear optical loop mirror using the nonlinear polarization rotation effect, *Opt Commun* 144 (1997), 60–64.
7. B.I. Escamilla, E.A. Kuzin, O. Pottiez, J.W. Haus, F. Gutierrez-Zainos, R. Grajales-Coutino, and P. Zaca-Moran, Fiber optical loop mirror with a symmetrical coupler and a quarter-wave retarder plate in the loop, *Opt Commun* 242 (2004), 191–197.

© 2006 Wiley Periodicals, Inc.

A COMPACT ORTHOGONAL TRIPOLARIZED MULTIAN TENNA WITH LOW MUTUAL COUPLING FOR MIMO CHANNEL MEASUREMENTS

Gang Yan, Zhengwei Du, and Ke Gong

Tsinghua University
Beijing 100084, China

Received 19 December 2005

ABSTRACT: A tripolarized multiantenna made up of three compact orthogonal dipoles is proposed. The three dipoles' phase centers are

compact within $1/6$ wavelength so that the spatial fading condition of the multi input multi output (MIMO) channel in subwavelength scale can be discriminated in three orthogonal directions of polarization by the multiantenna. © 2006 Wiley Periodicals, Inc. *Microwave Opt Technol Lett* 48: 1358–1362, 2006; Published online in Wiley InterScience (www.interscience.wiley.com). DOI 10.1002/mop.21658

Key words: multiantenna; tri-polarized; dipole; MIMO channel measurements; coupling

INTRODUCTION

Recent efforts aimed at improving available mobile communication capacity have generated interest in the polarization measurements of the multi input multi output (MIMO) wireless channel [1–3]. The channel measurements require the multiantenna to be incorporated with three independent antenna units in three orthogonal directions of polarization, respectively, each one of which has an omnidirectional H-plane pattern so as to receive the electric fields of incident waves coming from all directions. And since the application of multiantenna units integrated on one wireless handset is studied, the spatial-fading condition of the environment in subwavelength scale is of concern in MIMO channel measurements. Therefore, in order to discriminate the wireless channel's space fading on a small scale, the antenna units' phase centers ought to be as compact as possible for subwavelength measurement. In real MIMO systems, spatial-polarization diversity has been achieved successfully by the tripolarized multiantennas proposed in [1, 4], but the antenna units of the multiantenna [1] are not compact within a wavelength, or without the omnidirectional H-plane pattern for all of the antenna units [1, 4]. Although the bipolarized dipoles proposed in [5, 6] are multiantenna with two orthogonal units of omnidirectional H-plane pattern, the MIMO channel cannot be measured in three directions of polarization simultaneously by the two independent dipoles. So, a novel tripolarized multiantenna made up of three compact printed dipole antennas is proposed in this paper for real-time MIMO channel measurements. Usually mutual coupling between close antenna units is strong, so low mutual coupling between the multiantenna's units is an important feature of the multiantenna in order to maintain the channel's spatial correlation property for accurate MIMO channel measurements. However, when the third dipole antenna is integrated into the multiantenna (including two orthogonal dipole antennas already integrated), although the third dipole is orthogonal to the former two dipoles, the strong interference between the third one and the feed networks of the former two makes it difficult to arrange the third one compactly. Since mutual coupling is a barrier that has to be overcome from the bipolarized multi-antenna to the tripolarized multiantenna, insight as to how the three printed antennas and their feed networks are arranged is introduced in order to develop a methodology for achieving a compact, low-mutual-coupling multiantenna.

ANTENNA CONFIGURATION

The proposed tripolarized multiantenna is made up of three units: two horizontal planar dipoles (H-D1, H-D2) and a planar vertical dipole (V-D). The three planar dipoles are built on 0.8-mm-thick substrates with relative permittivity of 4.4. The multiantenna configuration is shown in Figure 1. Each dipole consists of two metal layers: the top layer (wide solid lines) and the bottom layer (areas surrounded by dash lines). The dimensions of the metal layers and the substrates are listed in Table 1. H-D1 and H-D2 share the same geometrical sizes, except for the height of the baluns (d_1 or d_2) and the position of matching lines (h_1 or h_2).

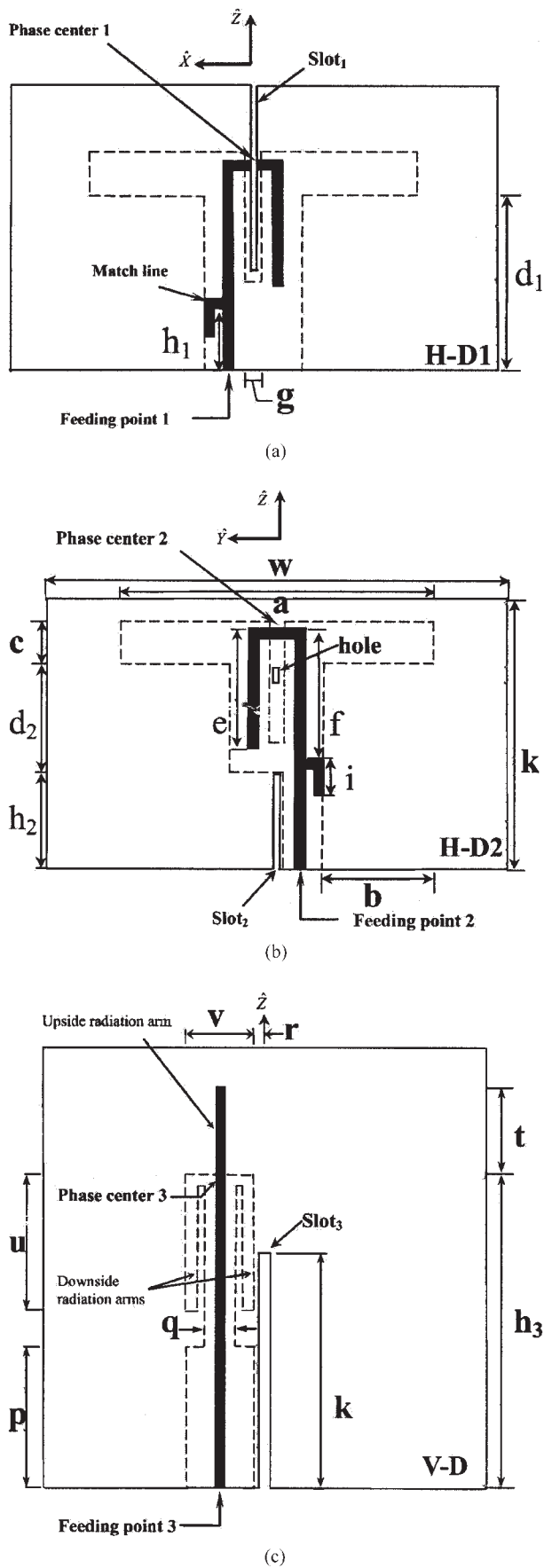


Figure 1 Geometry of the proposed multiantenna: (a) H-D1; (b) H-D2; (c) V-D

TABLE 1 Tripolarized Multiantenna Dimensions (All Dimensions in mm)

a	b	c	d_1	d_2	d_g	e	f	g	h_1
54	19	7	28	18.5	24	20.5	22.3	2.6	10
h_2	h_3	w	k	r	p	q	t	u	v
16.5	57	80	46	2	26	6	17.5	26.5	12

The two horizontal dipoles (H-D1, H-D2) are derived from the printed dipole antenna integrated with a balun of quarter-wavelength open-circuit stub [7, 8]. The microstrip via-hole balun [9] is not used for the more symmetric H-plane pattern obtained by using the open-circuit stub balun. The short “Γ” shape match line is designed for 50Ω match of the horizontal dipoles at resonant frequency (2.06 GHz), as shown in Figures 1(a) and 1(b). The phase centers of H-D1 and H-D2 are on the midpoints of their radiation arms. In order to assemble H-D1 and H-D2 orthogonally as well as arrange their phase centers compactly, 1-mm-wide slots, slot₁/slot₂, are cut on the H-D1 and H-D2, respectively, and a square hole is opened on the substrate of H-D2. Rotated 90° clockwise, H-D2 can be inserted into slot₁ on H-D1; meanwhile, the slot₁ on H-D1 seizes H-D2, as shown in Figure 2. Since the

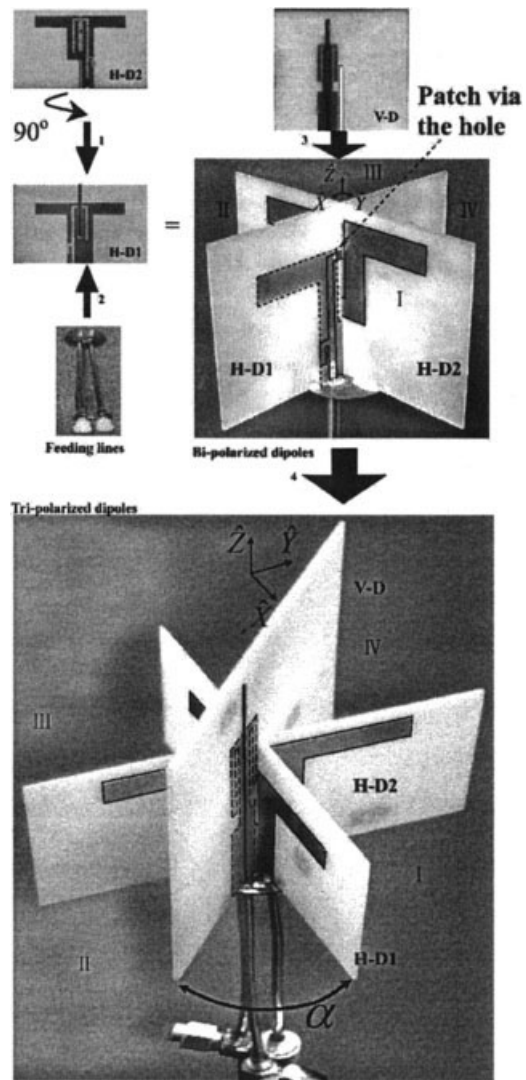


Figure 2 Assembly procedure of the proposed multiantenna

microstrip of the balun on H-D1 is cut off by the slot₁ at the point of phase center 1, the microstrip is patched via the hole after H-D1 and H-D2 have intersected each other to form right angles. The enlarged view of the patch via the hole is shown in Figure 3. V-D consists of an upside radiation arm and two downside radiation arms [10], as shown in Figure 1(c). The phase center of V-D is approximately at the midpoint of the upside and downside radiation arms. A 2-mm-wide slot, slot₃, is cut on the substrate of V-D so that the horizontal dipoles H-D1 and H-D2 can be inserted into slot₃ through their middle axis, axis \hat{z} , as shown in Figure 2. H-D1, H-D2, and V-D are mounted on the ground plate with diameter d_g , fed by three semirigid coaxial cables through feeding points 1, 2, and 3, respectively, as shown in Figure 4.

The procedure for assembling the proposed tripolarized multiantenna involves four steps, as shown in Figure 2. First, plug H-D2 in the slot₁ on H-D1, and then patch the cutoff microstrip line of H-D1 via the hole on H-D2. Second, solder the bottom layers of H-D1 and H-D2 on the ground plate to form a cross. H-D1 and H-D2 are fed at feeding points 1 and 2, respectively, and the outer conductor of the coaxial cables is soldered to the ground plate. Third, since H-D1 and H-D2 have divided the space into four quadrants, put V-D upright in quadrant II, away from H-D1 of 40° (α), as shown in Figure 2. Finally, solder the bottom layer of V-D on the ground plate with the coaxial cable feeding through feeding point 3. The top view of the three dipoles is shown in Figure 4.

LOW MUTUAL COUPLING DESIGN

V-D is arranged in quadrant II where the near fields stimulated by the dipoles and the baluns of H-D1 and H-D2 are relatively weaker than that in the other quadrants. Thus, mutual coupling between V-D and the baluns of H-D1 and H-D2 is reduced by placing V-D in quadrant II. The spacing from the phase center of H-D1 to that of H-D2 is 7 mm ($d_2 + h_2 - d_1$). The spacing from the phase center of V-D to that of H-D2 is 17 mm:

$$\sqrt{[h_3 - (c + d_2 + h_2)]^2 + \left[r + \frac{v}{2}\right]^2}$$

The height h_3 of V-D and the spacing r from the right side of V-D's bottom layer to axis \hat{z} are sensitive design parameters, which ought to be optimized for the compact phase centers of the multiantenna. Smaller h_3 and r make the three dipoles more compact; however, the axis-symmetric radiation pattern of V-D is distorted. Meanwhile, the interference of the near field of the three planar antennas increases the mutual coupling. In this design, the



Figure 3 Enlarged view of the patch via the hole

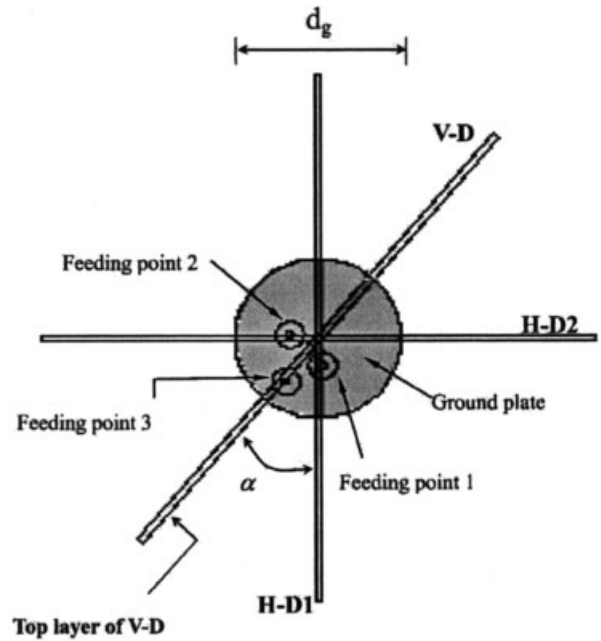
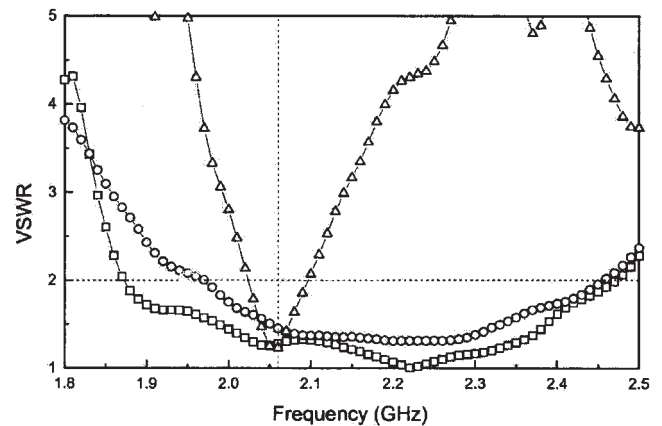
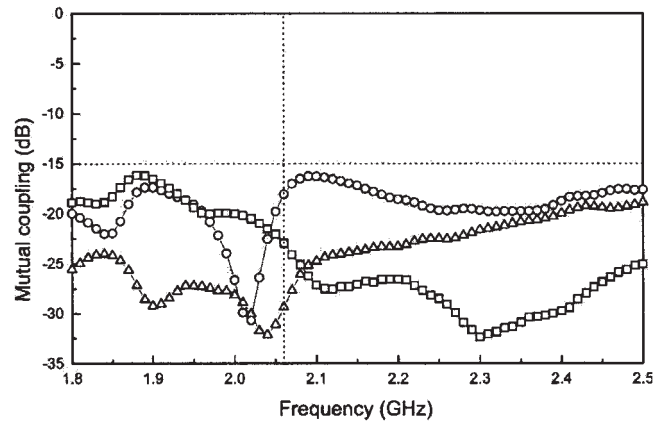


Figure 4 Top view of the proposed multiantenna



(a)



(b)

Figure 5 Measured VSWR and mutual coupling of each dipole antenna of the proposed multiantenna for port 1 (H-D1), port 2 (H-D2), and port 3 (V-D): (a) VSWR (—□—) VSWR1, —○— VSWR2, —△— VSWR3; (b) mutual coupling (—□— S_{12} ; —○— S_{13} , —△— S_{23})

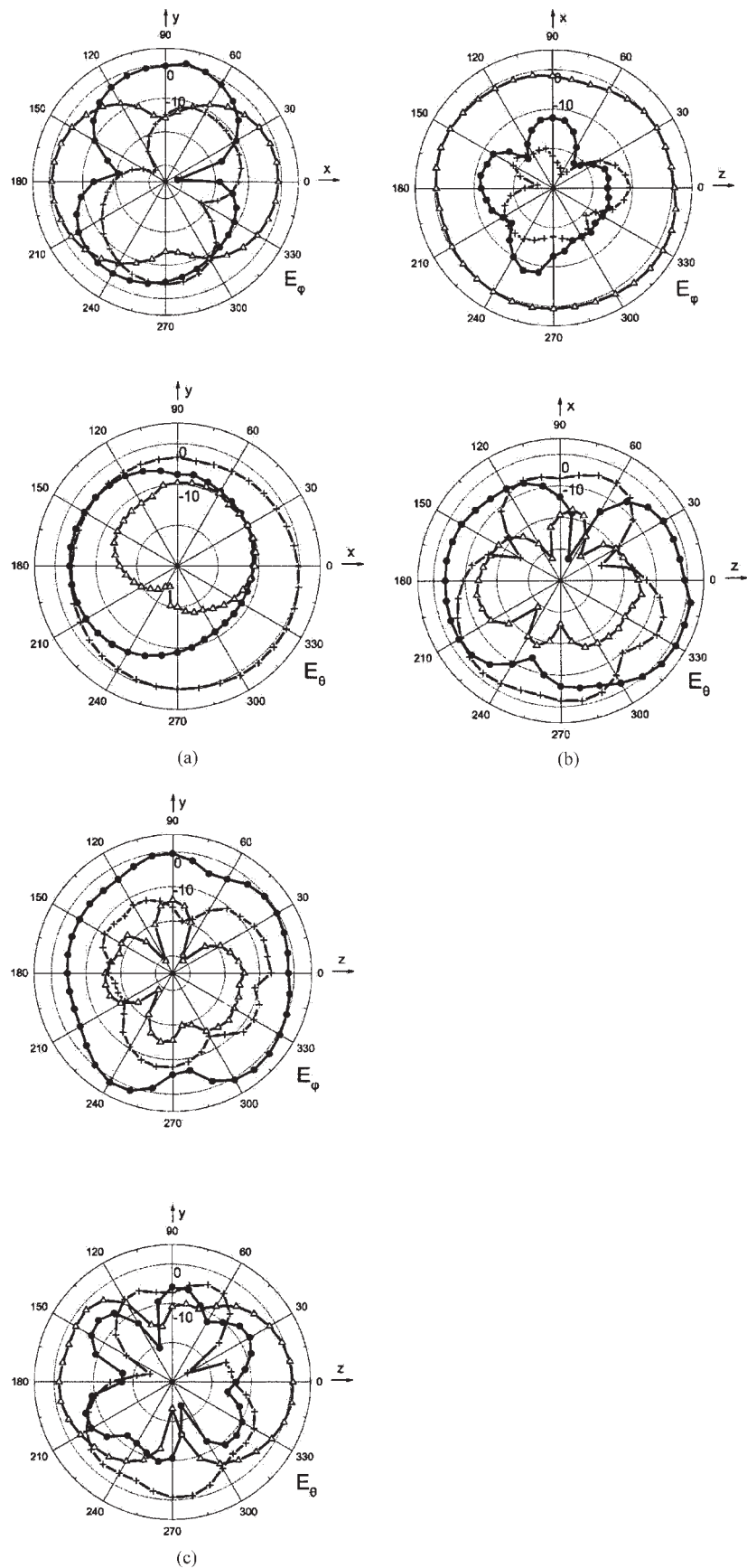


Figure 6 Measured antenna gain for each dipole antenna of the proposed multiantenna (—●— H-D1, —△— H-D2, —+— V-D): (a) E-plane of H-D1 and H-D2, H-plane of V-D (x - y plane); (b) H-plane of H-D2, E-plane of H-D1 and V-D (x - z plane); (c) H-plane of H-D1, E-plane of H-D2 and V-D (y - z plane)

optimized spacing between the phase center of H-D1 to that of V-D is 24 mm, within 1/6 wavelength at 2.06 GHz.

Since the near fields of the three printed dipole antennas are closely orthogonal, the mutual coupling between them is mainly caused by the ground-current interference. The metal layers of the three antennas are arranged to never intersect except where soldered on the ground plate, so no close current circle exists between the three dipole antennas. Therefore, although the three dipoles are arranged compactly and resonate at the same frequency, low mutual coupling between the three antennas is achieved.

RESULTS

The voltage standing wave ratio (VSWR), mutual coupling, and radiation patterns of each antenna of the proposed multiantenna have been measured. When one antenna is measured, the other two are connected with the 50 Ω matching load. H-D1 and H-D2 both operate from 1.95 to 2.45 GHz with a bandwidth of 22.7% (VSWR < 2), as shown in Figure 5(a). V-D is a narrowband antenna, operating at 2.06 GHz, with a bandwidth of 3.6%, 75 MHz (VSWR < 2). Each bandwidth of the multiantenna is wider than a channel for UMTS, so it is used for MIMO channel measurements in the UMTS band. Since the three dipoles are so compact, mutual coupling between the dipole antennas are measured below -15 dB, as shown in Figure 5(b). The measured gains for each printed antenna are shown in Figure 6. The H-plane pattern of each printed antenna is omnidirectional and the E-plane pattern is close to that of an ideal dipole antenna. The gains of the three dipole antennas on their H-planes are approximately 0 dB. The multiantenna can be used to discriminate the electric fields on three orthogonal directions of polarization as three orthogonal ideal dipoles in the MIMO channel measurements.

CONCLUSION

A compact, low-mutual-coupling multiantenna with three orthogonal printed dipoles incorporated with baluns has been proposed for real-time MIMO channel measurements. The phase centers of the three printed antennas are compact in order to discriminate the space fading on a subwavelength scale in the channel measurements. The multiantenna is compact in profile geometry but exhibits low mutual coupling with each unit of the omnidirectional H-plane pattern and simple impedance matching to the feed line.

ACKNOWLEDGMENT

This work is supported by National Natural Science Foundation of China (No. 60496318), the "863" Hi-tech Research & Development Program of China (No. 2003AA123110) and Tsinghua-QUALCOMM Associated Research Plan.

REFERENCES

1. M.C. Mtumbuka and D.J. Edwards, Investigation of tri-polarized MIMO technique, *Electron Lett* 41 (2005), 137–138.
2. H.J. Li and C.H. Yu, Correlation properties and capacity of antenna polarization combinations for MIMO radio channel, *Proc AP-S 2* (2003), 503–506.
3. C.C. Martin, J.H. Winters, and N.R. Sollenberger, MIMO radio channel measurements: performance comparison of antenna configurations, *Proc VTC 2* (2001), 1225–1229.
4. N.K. Das, T. Inoue, T. Taniguchi, and Y. Karasawa, An experiment on MIMO system having three orthogonal polarization diversity branches in Multipath-rich environment, *Proc VTC 2* (2004), 1528–1532.
5. H.E. King and J.L. Wong, An experimental study of a balun-fed open-sleeve dipole in front of a metallic reflector, *IEEE Trans AP 20* (1972), 201–204.
6. G. Yan, Z.W. Du, and K. Gong, A compact low coupling orthogonal

bi-polarized multi-antenna for MIMO channel measurements, *Proc AP-S*, Washington DC, 2005, session 128.

7. N. Michishita, H. Arai, M. Nakano, T. Satoh, and T. Matsuoka, FDTD analysis for printed dipole antenna with balun, *Proc APMC* (2000), 739–742.
8. G.S. Hilton, C.J. Railton, G.J. Ball, A.L. Hume, and M. Dean, Finite-difference time-domain analysis of a printed dipole antenna, *Proc AP-S 1* (1995), 72–75.
9. H.R. Chuang and L.C. Kuo, 3D FDTD design analysis of a 2.4-GHz polarization-diversity printed dipole antenna with integrated balun and polarization-switching circuit for WLAN and wireless communication applications, *IEEE Trans MTT 51* (2003), 374–381.
10. K.L. Wong, F.R. Hsiao, and T.W. Chiou, Omnidirectional planar dipole array antenna, *IEEE Trans AP 52* (2004), 624–628.

© 2006 Wiley Periodicals, Inc.

WIDEBAND EMC CHIP ANTENNA FOR WLAN/WiMAX OPERATION IN THE SLIDING MOBILE PHONE

Chun-I Lin,¹ Kin-Lu Wong,¹ and Shih-Huang Yeh²

¹ Department of Electrical Engineering
National Sun Yat-Sen University
Kaohsiung 804, Taiwan

² Computer & Communications Research Laboratories
Industrial Technology Research Institute
Hsinchu 310, Taiwan

Received 20 December 2005

ABSTRACT: A wideband electromagnetic-compatible (EMC) chip antenna for application in the sliding mobile phone for WLAN/WiMAX dual-network operation is presented. The proposed EMC antenna is easily fabricated by mounting a metal pattern onto a foam base of $30 \times 6 \times 6 \text{ mm}^3$. The metal pattern comprises a radiating portion and a vertical ground plane. The radiating portion further consists of a shorted driven strip and a shorted parasitic strip, both of them together generating a wide bandwidth for 2.4-GHz WLAN operation (2400–2484 MHz) and 2.5-GHz WiMAX operation (2500–2690 MHz). The vertical ground plane functions as an effective shielding wall and allows the antenna to be in direct contact with nearby electronic components or conducting elements. Small variations on the performances of the proposed antenna for the sliding mobile phone in the slid-open (talk) and standby conditions are also obtained. © 2006 Wiley Periodicals, Inc. *Microwave Opt Technol Lett* 48: 1362–1366, 2006; Published online in Wiley InterScience (www.interscience.wiley.com). DOI 10.1002/mop.21657

Key words: mobile antennas; chip antennas; internal mobile phone antennas; EMC antennas; WLAN antennas; WiMAX antennas

1. INTRODUCTION

The sliding mobile phone [1–3] has recently been available on the market and is usually equipped with a large display, which makes it very attractive for wireless users. For this kind of mobile phone, there are two separate, but electrically connected, ground planes, which is quite different from the conventional bar-type mobile phone with a single main ground plane [4]. When the sliding mobile phone is in the slid-open (talk) condition, a larger effective ground plane is formed. On the other hand, for the sliding mobile phone in the standby condition, the effective ground plane is smaller. Due to the different effective ground plane sizes for the slid-open and stand-by conditions, large variations in the operating bandwidth of the conventional internal shorted patch antennas have been observed [1]. To overcome this problem, we present in this paper an EMC chip antenna for application in a sliding mobile phone.